Aeroelastic tailoring for gust load alleviation

Lancelot, Paul; De Breuker, Roeland

Publication date
2016

Document Version
Accepted author manuscript

Published in
Proceedings of the 11th ASMO UK/ISSMO/NOED2016 International Conference of Numerical Optimisation Methods for Engineering Design

Aeroelastic tailoring for gust load alleviation

Paul Lancelot[*] and Roeland De Breuker[†]

Faculty of Aerospace Engineering, Delft University of Technology, the Netherlands

This paper presents the results from the equivalent static load method applied to gust response optimisation of an aircraft wing. Through the different optimisation runs, it is assessed that gust load cases can be critical and are difficult to constrain with the sole use of static load cases. Several cases are evaluated with different gust parameters and wing boundary conditions. Effects of control efficiency and engine location are also studied.

I. Introduction

GUST encounter is among the most critical loads for an aircraft [1]. The increasing aspect ratio of modern commercial aircraft wings and the weight reduction effort, generally result into increased wing sensitivity to dynamic loads. Loads mainly come from atmospheric conditions (gust loads) and from the action of the pilot/flight computer to control the aircraft (manoeuvre loads). The idea of load alleviation is not new and such a system has been in operation since the 70s [2]. Lockheed engineers applied this technology on the C5 Galaxy to reduce fatigue load cycles on the wing structure as they had been underestimated during the design phase [3]. Therefore, load alleviation was used to save weight, because additional airframe reinforcement would have been needed otherwise. About the same time, Lockheed also implemented a similar system on its civil airliner, the L1011 Tristar, and nowadays, such features are common on civil aircraft to improve aircraft handling and passenger comfort [2]. In combination with active load control using ailerons and spoilers, the wing structure can also be tailored in such way that it will relieve itself from the loads. This is achieved by a redistribution of the aerodynamics forces inward, caused by negative local angle of attack toward the wing tip. Backward swept wing genuinely exhibit this behaviour and the use of composite material can improve it furthermore. This was demonstrated in the work done by *Dillinger et al.* [4]. More generally, aeroelastic tailoring with composite materials has been a topic of research for many years now [5].

In an industrial context, specific requirements are provided in the certification. It covers constraints related to structural strength and stiffness, aeroelastic instability (flutter, divergence) and minimum control effectiveness over the entire flight envelope. All civil aircraft must be able to comply, and yet be as light as possible. The certification provides static load cases and dynamic ones. However the structural sizing process is mostly driven by fixed loads and by aeroelastic instability constraints [6]. Taking dynamic load cases earlier in the design process could be beneficial in term of performance, as the work done by *Kenway et al.*[7] shows that a wing optimised for fixed loads can failed when subjected to transient gust. However the main issue remains that these loads are generally dependent over the design itself. They are constantly changing during the optimisation, as the design evolve with it. Transient responses can also be computationally demanding and therefore costly to implement into current design optimisation process.

In this paper, the structural optimisation process of a wing that is designed for passive gust load alleviation is presented. To perform this optimisation, a gradient-based approach is preferred as the number of design variables is relatively large (≈180). However the computation of required sensitivity over a transient response is not an easy task [8]. The equivalent static loads (ESL) method formalised by *Kang et al.* [9] is used to bypass this issue and provides optimised results for static and dynamics load cases. In the present work the method is used with little improvement regarding the original idea as described in the next section. Nonetheless, it is worth mentioning that examples of improved ESL method exist in the literature. For instance, load sensitivities can be derived using a first order Taylor expansion at each coupling iteration, in order to approximate the loads at the next steps and hence accelerate the convergence [10]. *Bettebghor et al.* proposed a different approach based on surrogate

Communicating Author: P.M.G.J.Lancelot@tudelft.nl
[*] PhD Candidate.
[†] Assistant Professor.

modelling [8]. Both of these works were applied to engine pylon sizing in the event of a "fan blade off", a highly dynamic load case. ESL was extended to different scenarios, most of them summarized by *Park* [11]. These include non-linear geometries, multi body dynamics, and crash and topology optimisation for the automotive industry.

The paper will first introduce a brief description of the optimisation mythology and then highlight how the wing structural sizing can be influenced by various parameters. These parameters are the different gust cases, the wing boundary conditions, the location of the engine along the span and the minimum control efficiency value.

II. Optimisation methodology

The optimisation process is built around the equivalent static load method. ESL relies on a weak coupling between the transient simulations and the optimiser. To reach convergence it requires several iterations where loads are updated along the new design. This method has the advantage to be easy to implement regardless of the different tools used in the loop. It can take advantage of already existing gradient based optimisation and aeroelastic analysis code and was already applied to similar aero structural problems where gust loads are introduced in the optimisations [12,13,14]. The governing equation that needs to be solved for a gust analysis is the following:

$$M(x)\ddot{u}(t) + K(x)u(t) = f_{gust}\left(v_\infty, v_{gust}(t), \ddot{u}(t), \dot{u}(t), u(t)\right) \tag{1}$$

where u is the nodal displacement vector, M and K respectively the mass and the linear stiffness matrices which are dependent upon the design variables x and f_{gust} the aerodynamic forces due to a gust. Finally, v_{gust} is the vertical speed component of a transient gust and v_∞ the flow speed in the far field. No structural damping is required as the damping forces are provided by the aerodynamic part. Once the displacements computed from Eq. (1), a set of equivalent static loads f_{eq} can be retrieved from the time steps identified in the elements strain history as the most the critical:

$$f_{eq} = K(x)u(t_i) \tag{2}$$

In the case of a free flying aircraft simulation, the structural displacements are obtained by removing the rigid body translations and rotations from the displacement vector of each grid points.

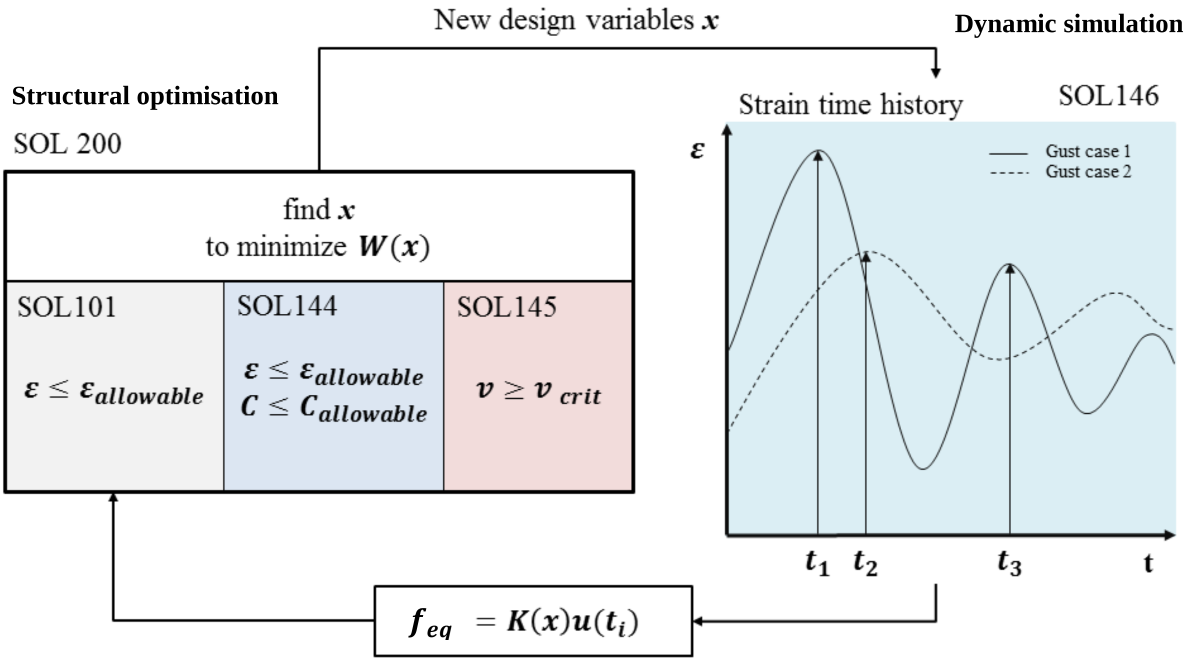

Figure 1: Schematic of the ESL method with the different NASTRAN solutions working together. The overall process in managed by a MATLAB script.

In the following example, described Figure 1, the loads are computed at each iteration with the transient aeroelastic module of NASTRAN, designated as the Solution 146 [15]. This solution relies on the Doublet Lattice Method (DLM) to solve the gust analysis problem. Although Eq. (1) is given as time dependent, NASTRAN solves everything in the frequency domain before converting the output results (displacement, strains etc.) in the time domain. This method is limited to linear aerodynamic and structural computation only.

Once the set of ESL generated, they are sent to the optimiser module of NASTRAN (SOL200) to be treated as a static structural optimisation problem. SOL200 can also account for steady aeroelastic and flutter constraints, which are computed by the SOL144 and SOL145 NASTRAN modules. For these responses the optimiser can derived sensitivities and efficiently performed gradient based optimisation [16]. In this example the constraints are applied on strength ($\varepsilon_{allowable}$), minimum static aileron efficiency ($C_{allowable}$) and minimum critical instability speed (v_{crit}). Buckling is not taking into account in the present work, although the authors acknowledge the influence that could have such constraints on the design and plan to implement it in future work.

The design variables used here are the panels' thickness (36 in total) and the laminations parameters. This formulation has been first introduced by *Tsai et al.* [17] and is used as a representation of the [A,B,D] stiffness matrix from the classical lamination theory. As the optimisation is only done for the in-plane response (tension, compression and shear), only 4 laminations parameters per panel are necessary to fully describe any symmetrical stacking sequences. Laminations parameters are denoted V_1, V_2, V_3, V_4 and present the advantage to be continuous compared to discrete ply angles. This continuous formulation greatly helps the optimiser to perform its task but doesn't directly define a proper stacking sequence. This is usually done as a post processing step using a genetic algorithm, but is not achieved in the present work. Nonetheless, the retrieval of a feasible stacking sequence greatly influences the optimised results and will be included in a future work [18].

Using a continuous formulation also requires using appropriate constraints for maximum strain. As the fibres orientations remain unknown, it is impossible to properly predict the actual failure envelope of a stacking sequence solely defines by its stiffness property. *IJsselmuiden et al.* [19] proposed a formulation of the widely used Tsai-Wu failure criteria for the continuous optimisation, by defining the area of the failure envelope common to all the plies angle. This criterion is used for in the present work, but with a safety coefficient of 2, as shown on Figure 2. This is to avoid having an optimised wing too flexible and therefore with a non-linear behaviour. It is interesting to note that carbon fibre laminate has much more strength in compression that in tension, the effect of this can be seen in the optimisation results section 5.

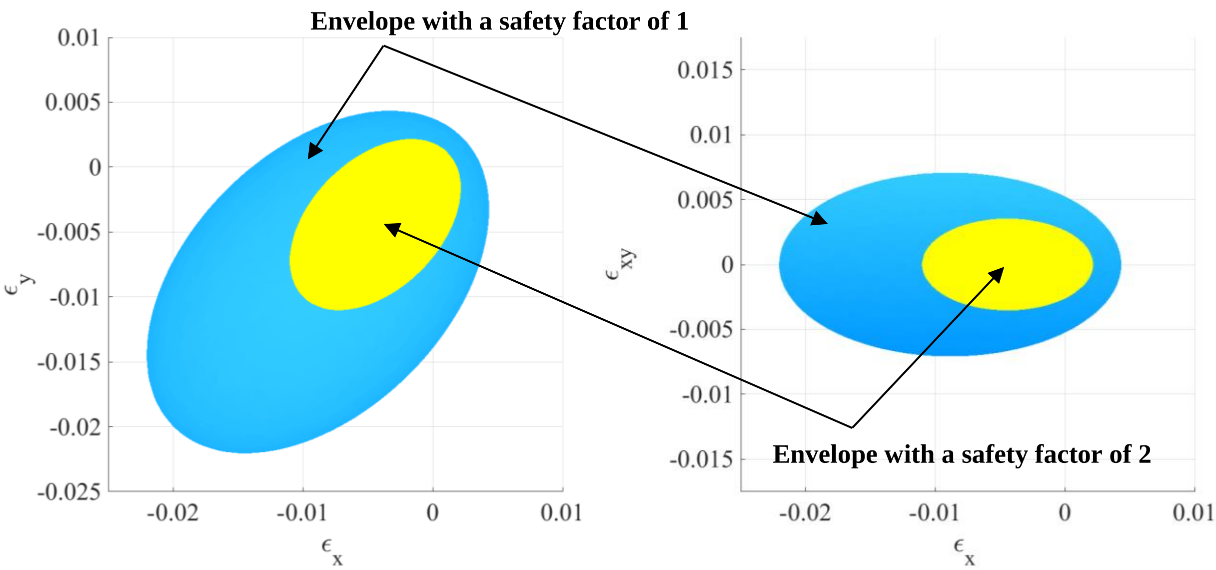

Figure 2: In plane failure envelope for Carbon-Epoxy (IM6). The methodology to compute these is detailed in the work by *IJsselmuiden et al.* [19].

Flutter and static divergence are constrained up to speed of 220 m/s. However due to the wing geometry, these constraints weren't active and thus their influence not discussed in this paper. Control efficiency is also taken into account for some of the optimisation example. Control efficiency reflects how much root bending moment Mcan be obtained from a specific aileron deflection on a flexible wing. A 100% value represents the moment created by an aileron mounted on a rigid wing. This constrained is only used on static cases.

$$C_{allowable} = \frac{M_{Flex}}{M_{Ref}}$$

III. Model description and load cases

The aircraft model used for this study is a 90 seats regional turboprop, derived from existing model such as the ATR72 or the Bombardier Q400. The choice of such configuration is motivated by the current research done on this aircraft type within Clean Sky 1 & 2 [20]. Furthermore, as DLM method is used to compute the aerodynamic loads, a subsonic aircraft was preferred over a transonic configuration. The task of assigning specific aircraft data can seems arbitrary; however the mass properties need to be taken into account for the dynamic load cases. Therefore coherent model data are necessary to ensure valid results that could be extrapolated to more accurate model.

Wing span	30 m
Fuselage length	30 m
Wing surface	75 m^2
Wing aspect ratio	12
Mean aerodynamic chord	2.5m
Nominal Mach	0.6
Nominal altitude	25000ft
Fuselage + Tail empty weight	5t
Engine weight	1.5t × 2
Wing weight (ribs, LE/TE, flaps etc.)	2.05t × 2
Wing weight (skins and spars)	1t x 2
Total empty weight	14.1t
Maximum take-off weight	30t
Fuel weight	3.075t × 2
Pax and cargo weight	9.75t

Table 1: Weight and dimensions for the full aircraft. Note that the weight from the wing skins and spars can vary during the optimisation.

The FEA model is built of 801 CQUAD4 shell elements, 123 CONM2 concentrated mass and 41 RBE2 rigid body elements. Wing skins and spars are made of the CQUAD4 elements, while the ribs are defined by the RBE2 elements. Therefore the ribs properties are not optimized. This also reduces the number of degrees of freedom of the structure, as grid points on the same rib have the same displacement. Therefore, the size of the stiffness matrix K that needs to be extracted from the model is only 246 × 246. The inertia properties of the fuselage are embedded within the concentrated mass card located at the centre of gravity of the aircraft.

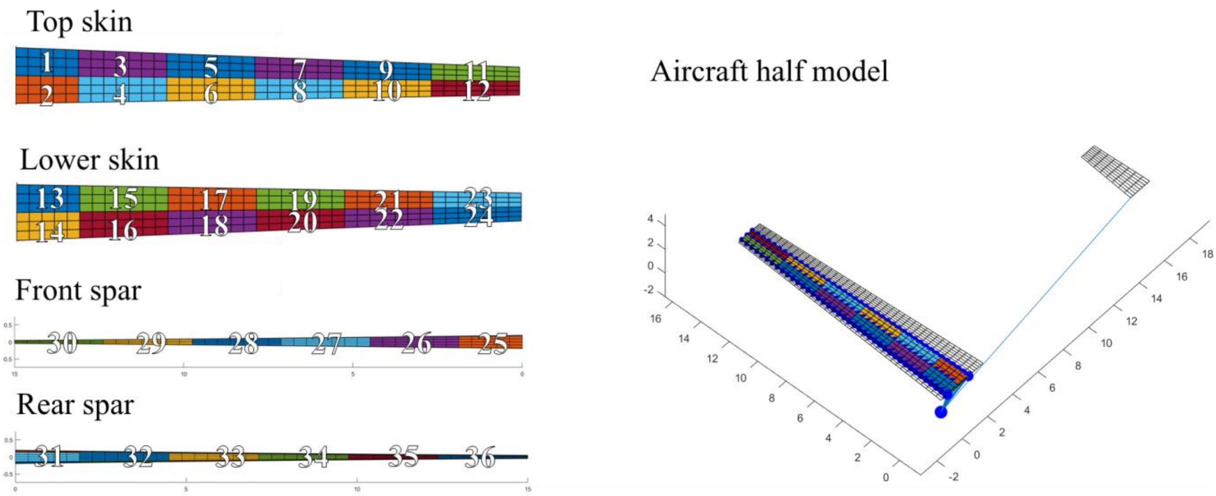

Figure 3: FEA model of the aircraft. The blue spheres represent the distributed concentrated mass. Numbers represent the panel properties IDs.

The Certification Specification 25 for large aircraft issued by EASA specifies “1-cos” gusts an aircraft needs to sustain [21]. The gust loads have to be defined with a half wave-length going from 9 to 110m. The gust amplitude is actually a function of its wave-length and altitude at which the aircraft is flying. Finding the critical gust cases over the entire flight envelope is a tricky matter as it requires to run many simulations, but recent work involves the use of reduced order model to solve that issue [22]. For the sake of simplicity, four gust cases are selected as the dynamic loads in this paper. The altitude, fuel loading and speed remain constant.

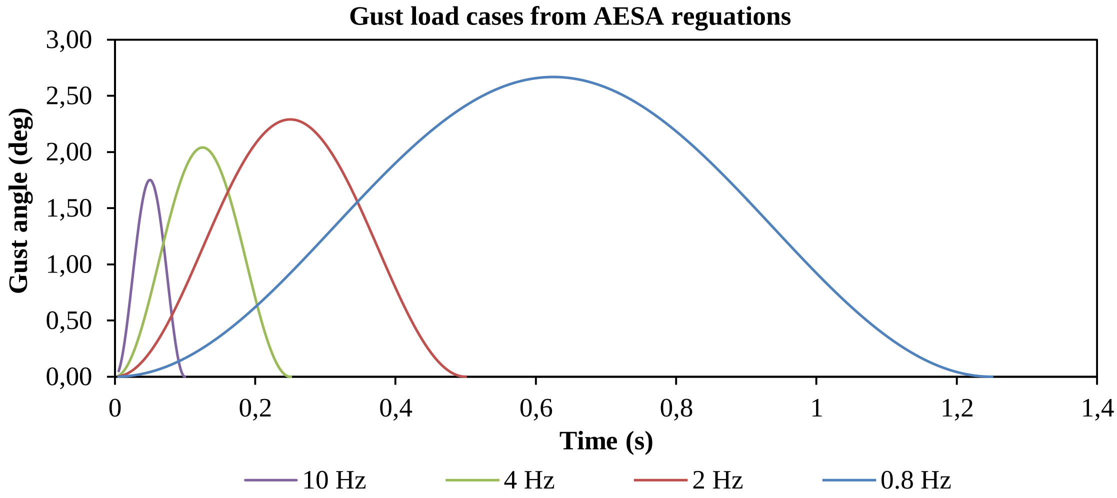

Figure 4: Gusts vary in amplitude and speed.

In addition to the gust load cases, static load cases are also applied. The static 2.5g load case is a well-known requirements used for aircraft structure certification. In the present work, an angle of attack of 4 degrees is sufficient to lift 30t of weight at cruise condition. The trim angle for the 2.5g load case is therefore about 10 degrees. Additional static load cases are used in some optimisation run to evaluate how they influence the tailoring. These static load cases and the associated angle of attacks are fixed during the optimisation. Dynamic load cases have a trim set to 0.

Load case number	True air speed	Frequency	Static load factor (g)	Aileron deflection in rad (deg)	Gust amplitude in rad (deg)
Static load cases					
1	185 m/s	/	(0.01, 1.40, 2.50, 3.60, 4.60)	0	/
2	185 m/s	/	0	0.25 (14.3)	/
Transient load cases					
3	185 m/s	10 Hz	0	0	0.0306 (1.67)
4	185 m/s	4 Hz	0	0	0.0356 (2.02)
5	185 m/s	2 Hz	0	0	0.04 (2.28)
6	185 m/s	0.8 Hz	0	0	0.0466 (2.66)
Flutter/Divergence load case					
7	155 – 225 m/s	/	0	0	/

Table 2: Summary of the different load cases.

IV. Results

Several optimisations with different test cases were performed. Most aero structural optimisation is performed on a clamped wing but gust loads can also vary with the flight dynamic properties of the aircraft. As shown by *Reimer et al.* [23], a free flying aircraft will experience lower magnitude gust loads. The influence of the boundary conditions on the gust responses and on the resulting optimisation is assessed. By allowing the aircraft half model to freely move in pitch and plunge, it was possible to recreate the symmetrical aero elastic behaviour of a full aircraft. It can be seen on Figure 5 that a free wing will be subjected to less root bending moment for a “slow” gust at 0.8Hz. In this configuration however, the peak amplitude on the load is achieved not during the initial gust response, but when the wing is going down again. This illustrates that flight dynamic can have an influence on the loads. While the loads are lower, this can actually change the outcome of the optimisation, as the wing box isn’t stressed the same way. It must be noted that the use of active pitch control could modify the flight behaviour and therefore the loads as well. However no active control is implemented in the present work.

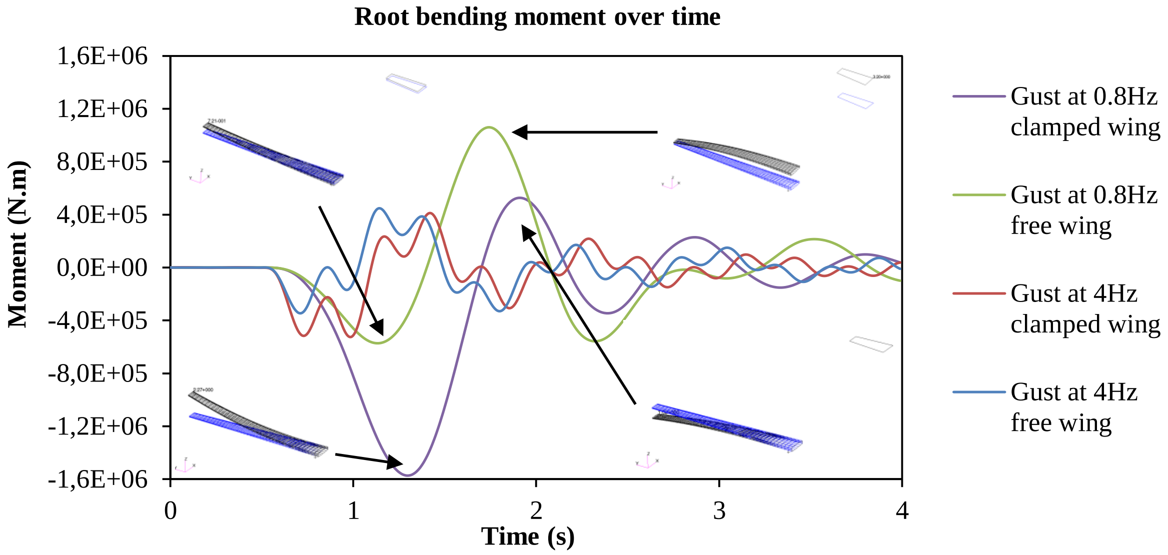

Figure 5: Root bending moment created by a gust encounter, for a clamped wing and a wing mounted on an aircraft with two degrees of freedom (pitch and plunge). All gusts start at 0.5 sec in the simulation.

If the wing is clamped, the maximum loads are going to be in tension in the lower skin and in compression in the top skin. Since buckling isn’t taken into account in the present work, composite panel are much stronger in compression than in tension. This results into lower thickness on the top skin. On the other hand, the free wing has its top skin stressed in tension which results in slightly higher thickness compared to the bottom skin on Figure 6. In term of weight, the optimised clamped wing is 6.7% heavier than the free wing as the plunge motion allows reducing some of the loads.

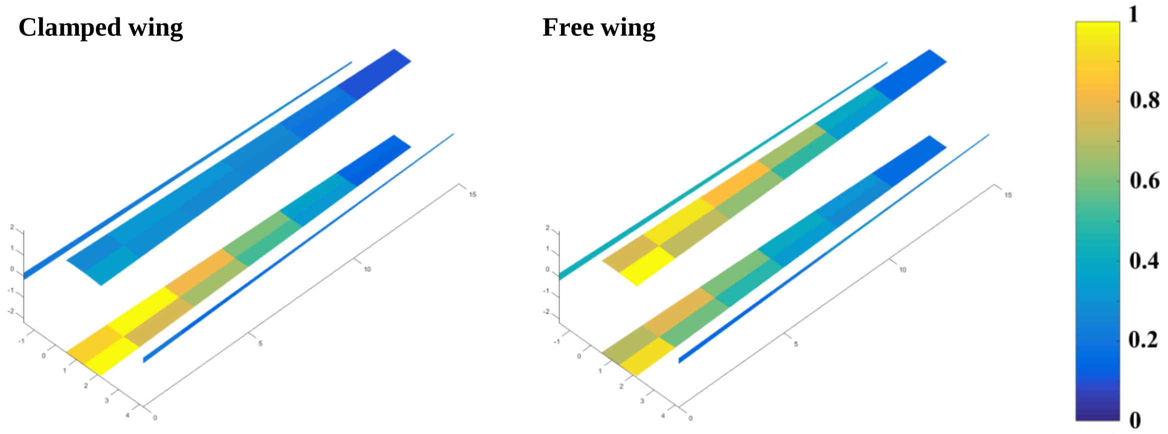

Figure 6: Normalised thickness distribution for two different configurations.

It can be noticed that the loads from “fast” gust are less impacted by the boundary conditions, and generate similar root bending moment. It is worth to mention that slow and fast gust don’t stress the wing at the same location. As shown on Figure 7, fast gusts tend to be more critical toward the wing tip, while slow one have more effect on the root. This is valuable information for whom designing wingtip devices for instance.

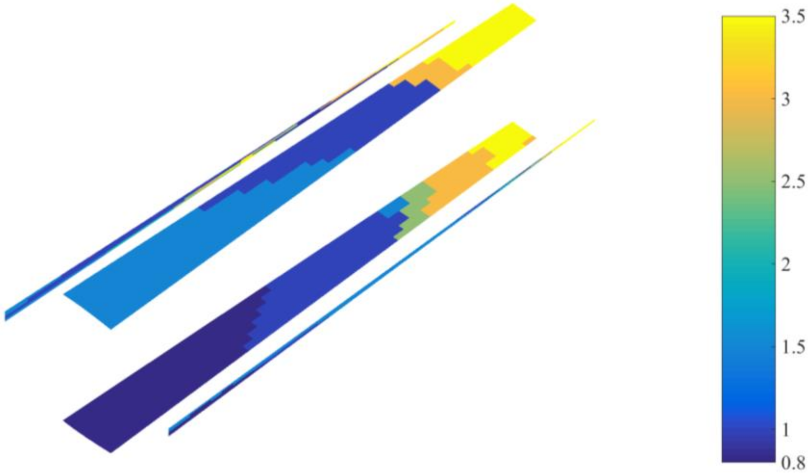

Figure 7: Criticality of different gust frequency (here in Hz) over the wing. This figure is obtained with additional load cases to better illustrate the dependency with the frequency.

Gust loads can be considered as flexible. Flexible loads are dependent over the design itself and can change during the optimisation as the design evolves. It also means that for the same gust and flight conditions, a stiff wing will more likely experience different loads compare to a flexible one. This is illustrated by running different optimisation problem, having the same gust cases, but with different static load conditions. Results on Figure 8 show the different constraints values for the different optimised design:

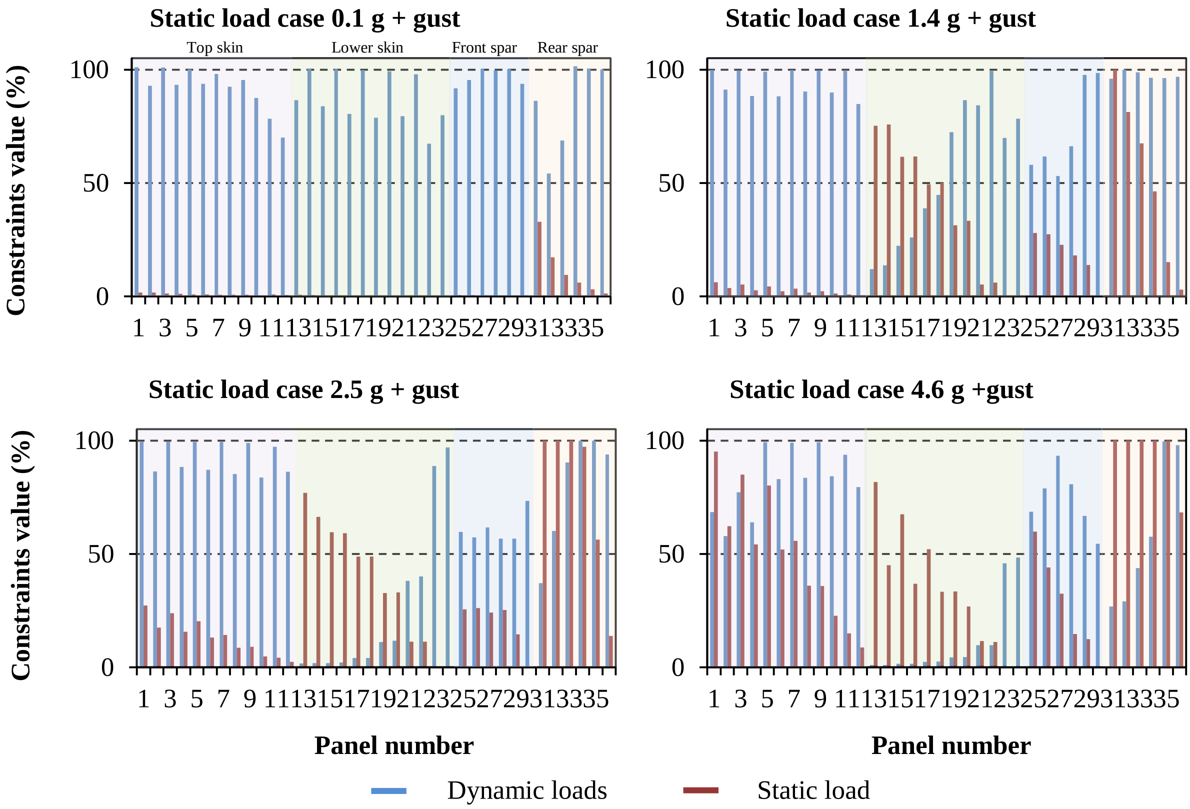

Figure 8: Constraint values for strength after optimisation.

Even with high static load some of the panels are more likely to be critical with respect of the dynamic loads. In this numerical experiment, the wing is free in pitch and plunge, therefore the top skin will be more critical to gust loads. On the other hand, the boundary conditions doesn’t have any impact on the static load case, therefore the lower skin is more likely to be sized by these loads. We can also see that it is more difficult to reach an optimised design which is fully stressed, as the optimiser as to deal with a broader spectrum of load cases. Indeed, a high static load case will lead to a very stiff wing, therefore more sensitive to fast gust cases toward the tip. When static load cases are removed, and the wing purely optimised for dynamic load cases, the wing tends have lower natural frequency because less stiff. When comparing the outcome of the different run, it is clear that a high static load case induced a final higher optimised weight. On Figure 9 we can see that fast gust load root bending moment slightly increase with weight, while the root bending moment from gust at 0.8 Hz is decreasing. This can be seen as the influence on the tailoring from static load case.

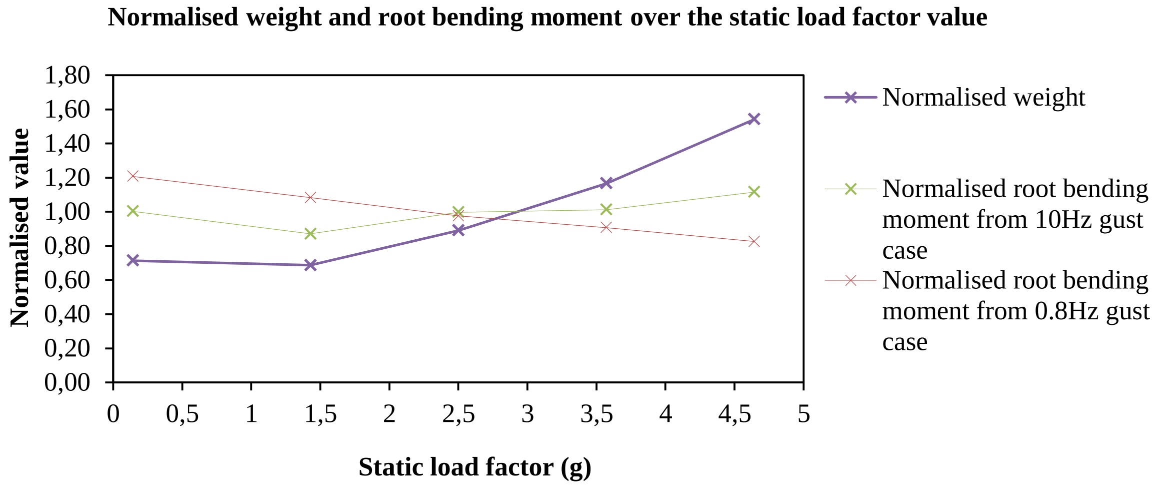

Figure 9: Summary of the weight and root bending moment of the different optimisation run.

As enunciated in chapter 2, the optimiser doesn't have the sensitivities, linking gust loads and design variables. However, for static aero elastic loads, NASTRAN is able to derive the appropriate sensitivities for such problem. Therefore, the optimiser will be able to aero elastically tailor the wing by inducing a negative twist distribution toward the tip in order to shift the lift inward, and therefore reduce root bending moment. This is achieved by moving the elastic centre toward the leading edge, usually by increasing the front spar thickness. If composite materials are used, the orientation of the fibres can also be used for that purpose. On Figure 10 we can see that once optimised for different static load cases and the gust loads, the optimised wing have a different behaviour under 2.5g. The one optimised for very high static loads will exhibit a negative twist distribution outward. On the other hands, the one optimised with only gust loads has the opposite behaviour. It can also be seen on both Figure 9 and Figure 10 that applying a small static load case is 1.4g has an effect on the optimised results.

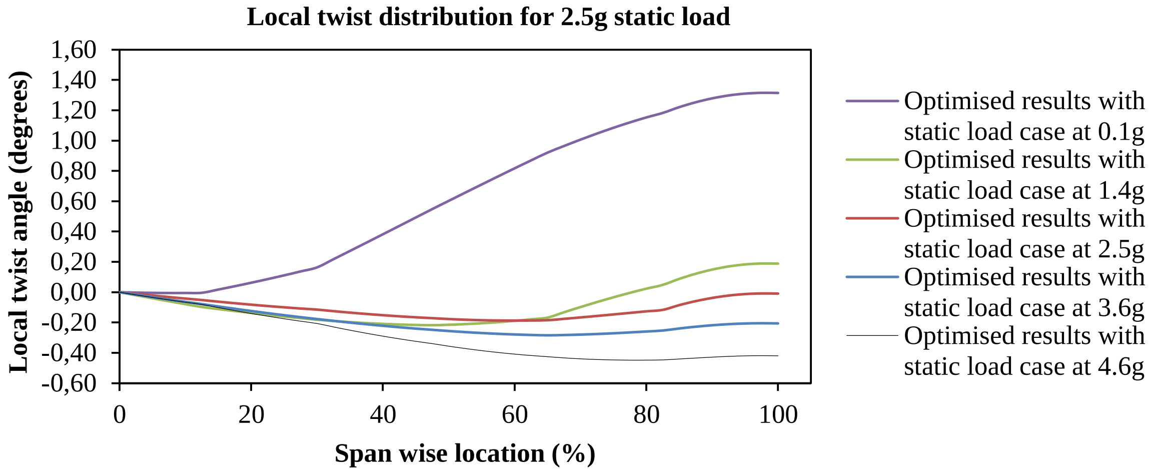

Figure 10: Local twist distribution for the different optimised results.

It is known that in order to reduce the root bending moment, engine and fuel can be shift outward to balance the lift. This is common practice in the aircraft industry and fuel system are design to accommodate such purpose, on the ground, and in flight [24]. Even if the engine location results in the trade-off between many parameters (such as the requirement to be able to take off with a single engine), the ability to optimise for dynamic loads revealed an interesting trade-off. A single point mass that accounts for the engine, its nacelle and the propeller is moved along the span, roughly 1m ahead the front spar position. The wing is clamped to remove any effect from the flight dynamic. Both gust and static (2.5g) cases are used to run the optimisation. The results on Figure 11 shows that having the engine under the wing is beneficial in term of weight when located up to 40% of the span, with a reduction of the static root bending moment. Regarding the dynamic cases, having this extra mass hanging under the significantly change its dynamic behaviour. The engine mid-wing also reduces the root bending moment in the case of gust at 0.8Hz while slightly increase it for a fast gust. For clarity gust loads at 2Hz and 4Hz are not displayed on the charts but exhibit similar behaviour. The overall weight penalty after moving the engine passed 50% of the span is a good indication on where the engine should and shouldn't be.

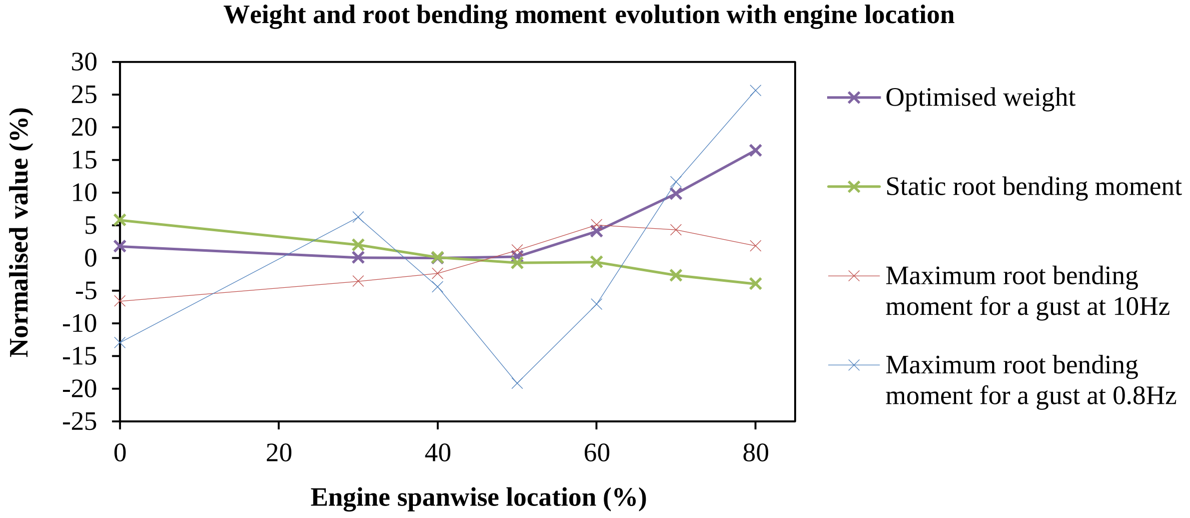

Figure 11: Summary of the weight and root bending moment of the different optimisation run.

Some optimisation cases were run with control efficiency as a constraint as well:

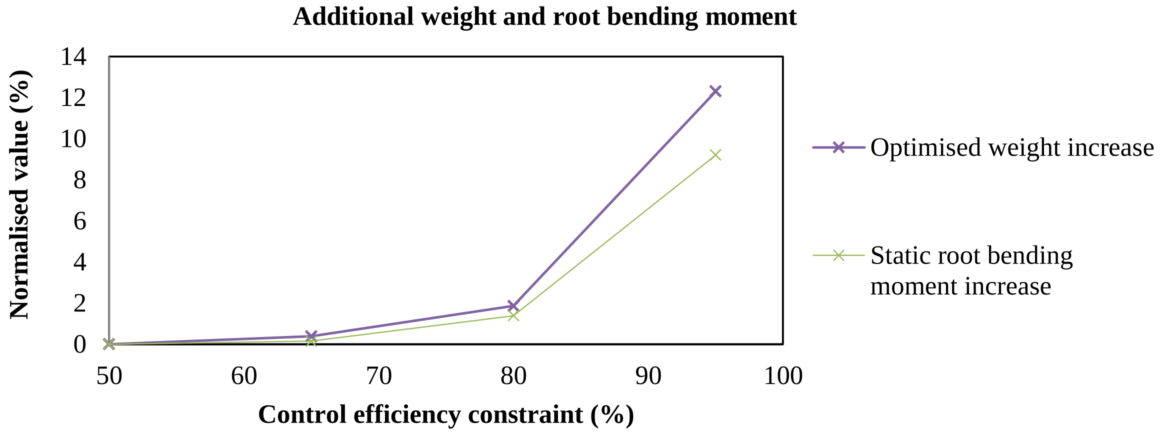

Figure 12: Summary of the weight and root bending moment of the different optimisation run.

On Figure 12 it is noticeable that trying to get close 100% aileron efficiency will require a stiffer wing (as shown on Figure 13), inducing more weight and lesser aero-elastic tailoring. As the present work only cover the control efficiency as a static load case, it already highlights the dilemma of having a very flexible wing, ideal to reduce gust loads passively, but with poor control effectiveness, requiring larger control surfaces, or the opposite.

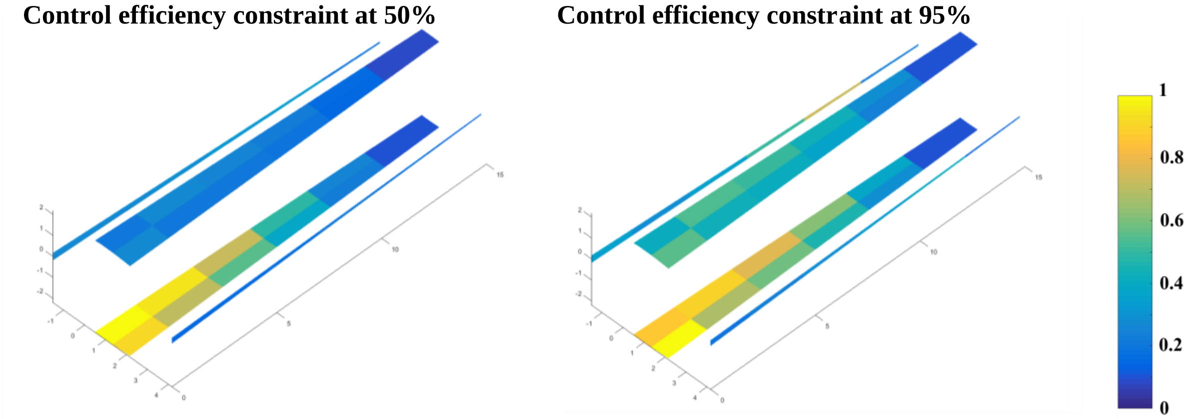

Figure 13: Normalised thickness distribution for two different configurations.

Regarding composite optimisation there are significant differences with the tailored results obtained by *Werter and De Breuker* [25] for instance, as these were obtained with static load cases only. Most of the tailoring appears to be done through thickness variations. In term of stiffness optimisation, as shown on Figure 14, the optimiser preferred to go for quasi-unidirectional laminates on the top and lower skin. This type of lay-up can in theory take very high loads in tension and compression. These results don't really vary as respect of different load cases or boundary conditions. On the spars we can see some variations in the stiffness. The laminates on the rear spars are most likely to have a stacking sequence close to [±45°]s, very stiff in shear loading condition. The results would probably be different if panel buckling and manufacturing constraints were taken into account [18].

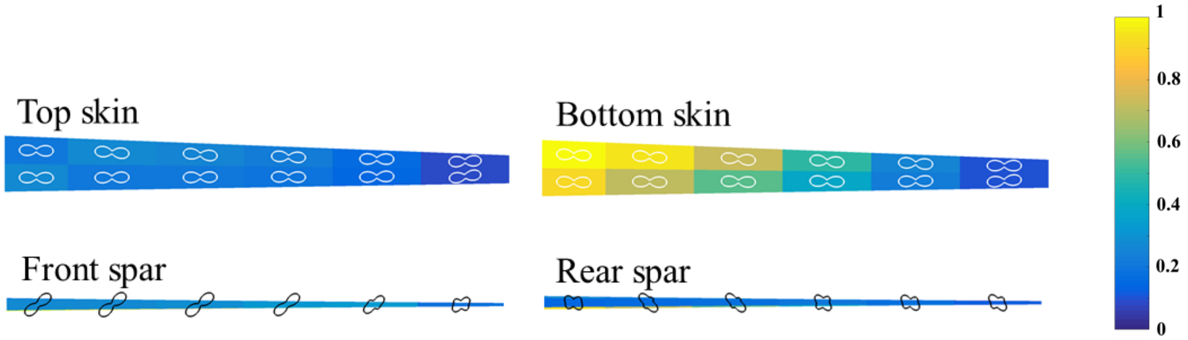

Figure 14: Stiffness distribution for two different configurations (the black and white shapes). The colour scale indicates the normalised thickness distribution.

The ESL method relies on a weakly coupled iterative scheme, convergence of the solution is therefore a major concern. The convergence rate and regularity of the optimisation results are related to many parameters. Among them, loads sensitivity to design changes between two iterations is critical. As shown on Figure 15, the use of an under relaxation factor can be a solution to help the convergence. In this scenario, the design variables x_i at the iteration n are multiply by 0.25 and added to 0.75 of the design variables at n_{-1}.

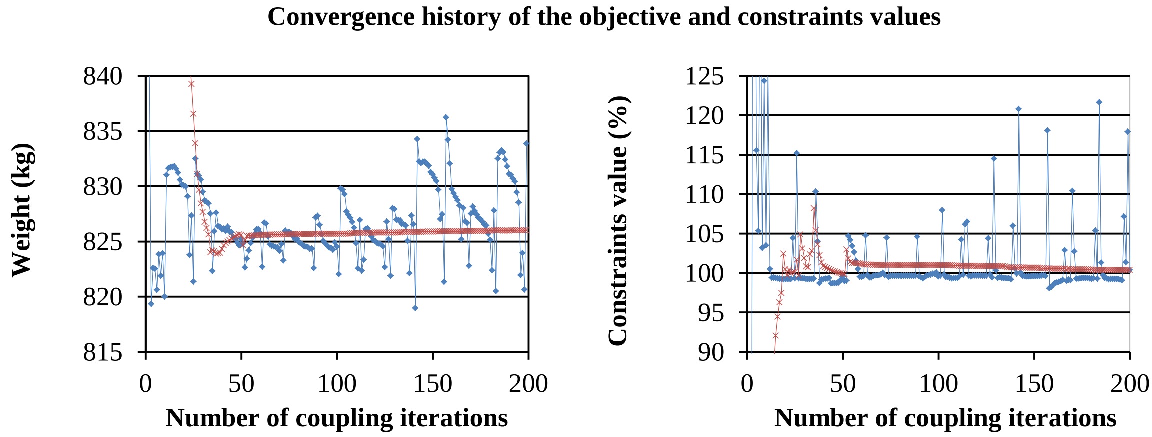

Figure 15: Red symbols are the results with under relaxation factor, and the blue ones without it.

Finally, as shown on Figure 8, 15 and 16, the ESL method is able to comply quite well with structural constraints. In the present work, only 36 design patches were optimised, therefore the final design cannot be fully stressed. However, by adding more design variables, this is something that could be reached with limited extra computational cost thanks to the use of a gradient based optimiser. It can also be shown with Figure 16 that loads tend to vary in space much quicker at the tip than at the root, meaning that the design patches would need to be smaller nearby the tip.

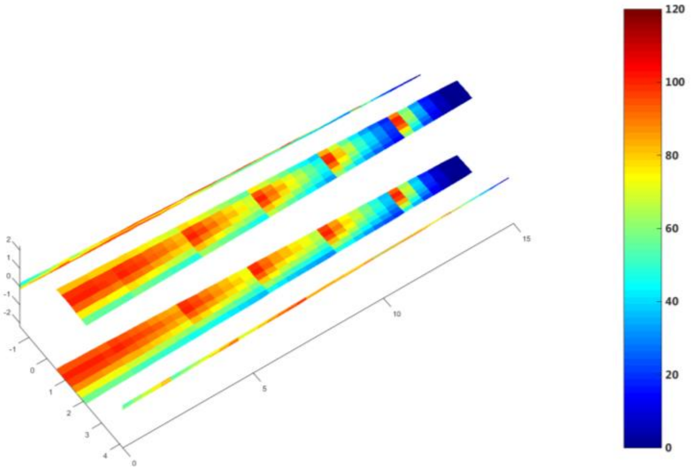

Figure 16: Maximum strength constraint value (%) for a wing optimised with dynamic loads.

V. Conclusion

This paper demonstrates that the ESL method can be applied to size aircraft wing structure for dynamic load cases. Through the different optimisation run, results shows that gust load cases can be critical for the structure and are difficult to constrain with the sole use of static load cases. Fast gust loads tend to be critical at the tip, slow ones at the root. One interesting matter is that the boundary condition of the wing (clamped or free flying) can affect the slow gust loads, but has a limited impact on the fast load cases. Most of the tailoring is done through the thickness distribution, rather than fibres orientations. Though, it is important to keep in mind that in the present work, only strength constraints are used for the structural sizing, therefore panel buckling, manufacturing constraints and other practical requirements related to composite structure are ignored. This will be included in a future work and will likely change the outcome of the optimisation. The ESL method also allows for interesting trade-off for the engine location. Finally this method can be implemented into an MDO framework and easily be combined with existing tools.

Acknowledgements

The work presented herein has been supported by funding from the People Programme (Marie Curie Actions) of the European Union’s Seventh Framework Programme FP7 2012 under REA Grant agreement n˚316394. It has also been funded by the European Community’s CleanSky 2 Programme under Horizon 2020 (H2020) under the Grant Agreement 686804. The ReLOAD project (Regional turboprop Loads control through active and passive technologies) is a CfP project funded under the Regional IADP involving 2 partners. The project started on 1 December 2015. Finally the authors would like to thank Dr. Terence Macquart from the University of Bristol and Marco Tito Bordogna from ONERA/TUD for their help on the editing of this paper.

References

[1]Hoblit, F.M. "Gust Loads on Aircraft: Concepts and Applications", American Institute of Aeronautics and Astronautics, 1988.

[2]Regan, C.D. and Jutte, C.V. "Survey of Applications of Active Control Technology for Gust Alleviation and New Challenges for Lighter-weight Aircraft", NASA technical report 216008, 2012.

[3]Disney, T. E. "C-5A Active Load Alleviation System", J. Spacecr. Rockets. 14, pp. 81–86, 1977.

[4]Dillinger, J.K.S., Klimmek, T., Abdalla, M.M. and Gürdal, Z. "Stiffness Optimization of Composite Wings with Aeroelastic Constraints", J. Aircr. 50, pp. 1159–1168, 2013.

[5]Jutte, C. and Stanford, B.K. "Aeroelastic Tailoring of Transport Aircraft Wings: State-of-the-Art and Potential Enabling Technologies", NASA technical report 218252, 2014.

[6]Grihon, S., Krog, L. and Bassir., D. "Numerical Optimization applied to structure sizing at AIRBUS A multi-step process", Int. J. Simul. Multidisci. Des. Optim. 3, pp. 432-442, 2009.

[7]Kenway, G., Kennedy, G. & Martins, J. " Aerostructural optimization of the Common Research Model configuration", in proceeding of 15th AIAA/ISSMO Multidisciplinary Analysis and Optimization Conference, American Institute of Aeronautics and Astronautics, Atlanta, GA, 2014.

[8]Bettebghor, D. and Blondeau, C. "Prise en compte de la flexibilité des cas de charges dimensionnants en optimisation de structure", in proceeding of 11e Colloque National en Calcul des Structures, Giens, 2013.

[9]Kang, B. S., Choi, W. S. & Park, G. J. "Structural optimization under equivalent static loads transformed from dynamic loads based on displacement", Comput. Struct. 79, pp. 145–154, 2001.

[10]Grihon, S. "VIVACE" project final report, pp. 36, 2007.

[11]Park, G.-J. "Technical overview of the equivalent static loads method for non-linear static response structural optimization", Struct. Multidiscip. Optim. 43, pp. 319–337, 2010.

[12]Daoud, F., Petersson, O., Deinert, S. and Bronny, P. "Multidisciplinary Airframe Design Process: Incorporation of steady and unsteady aeroelastic loads", in proceeding of 12th AIAA Aviation Technology, Integration, and Operations (ATIO) Conference and 14th AIAA/ISSMO Multidisciplinary Analysis and Optimization Conference, American Institute of Aeronautics and Astronautics, 2012.

[13]Wildschek, A., Haniš, T. and Stroscher, F. "L_∞-Optimal feedforward gust load alleviation design for a large blended wing body airliner", Progress in Flight Dynamics, GNC, and Avionics. 6, pp. 707-728, 2013.

[14]Kim, Y.I., Park, G.J., Kolonay, R.M., Blair, M. and Canfield, R.A. "Nonlinear Dynamic Response Structural Optimization of a Joined-Wing Using Equivalent Static Loads", J. Aircr. 46, pp. 821–831, 2009.

[15]MSC.Software Corporation. MSC Nastran 2014 Aeroelastic Analysis User's Guide, 2014.

[16]MSC.Software Corporation. MSC Nastran 2012 Design Sensitivity and Optimization User's Guide, 2012.

[17]Tsai, S.W. and Pagano, N.J. "Invariant properties of composite materials", Def. Tech. Inf. Cent., 1968.

[18]Macquart, T., Bordogna, M.T., Lancelot, P. and De Breuker, R. "Derivation and application of blending constraints in lamination parameter space for composite optimisation", Compos. Struct. 135, pp. 224–235, 2016.

[19]IJsselmuiden, S.T., Abdalla, M.M. and Gürdal, Z. "Implementation of strength based failure criteria in the lamination parameter design space", AIAA J. 46, pp. 1826–1834, 2008.

[20]Regional Aircraft | Clean Sky. Available at: http://www.cleansky.eu/content/page/regional-aircraft

[21]European Aviation Safety Agency. Certification Specifications Large Aeroplanes, Amendment 18, 2016.

[22]Castellani, M., Lemmens, Y. & Cooper, J. E. "Parametric reduced-order model approach for simulation and optimization of aeroelastic systems with structural nonlinearities" Proc. Inst. Mech. Eng. Part G J. Aerosp. Eng., vol. 230 no. 8, pp. 1359-1370, 2015.

[23]Reimer, L., Ritter, M., Heinrich, R. & Krüger, W. " CFD-based Gust Load Analysis for a Free-flying Flexible Passenger Aircraft in Comparison to a DLM-based Approach", in proceeding of 22nd AIAA Computational Fluid Dynamics Conference, American Institute of Aeronautics and Astronautics, 2015.

[24]Langton, R., Clark, C., Hewitt, M. and Richards, L. "Aircraft Fuel Systems", Wiley, 2009.

[25]Werter, N.P.M. and De Breuker, R. "A novel dynamic aeroelastic framework for aeroelastic tailoring and structural optimisation", Compos. Struct. 158, pp. 369–386, 2016.